



**HAL**  
open science

## Optical and electrical diagnostics in an iodine plasma

Florian Marmuse, Romain Lucken, Cyril Drag, Jean-Paul Booth, Anne Bourdon, Pascal Chabert, Ane Aanesland

► **To cite this version:**

Florian Marmuse, Romain Lucken, Cyril Drag, Jean-Paul Booth, Anne Bourdon, et al.. Optical and electrical diagnostics in an iodine plasma. 36th International Electric Propulsion Conference (IEPC 2019), Sep 2019, Vienne, Austria. hal-02341690

**HAL Id: hal-02341690**

**<https://hal.science/hal-02341690>**

Submitted on 18 Mar 2021

**HAL** is a multi-disciplinary open access archive for the deposit and dissemination of scientific research documents, whether they are published or not. The documents may come from teaching and research institutions in France or abroad, or from public or private research centers.

L'archive ouverte pluridisciplinaire **HAL**, est destinée au dépôt et à la diffusion de documents scientifiques de niveau recherche, publiés ou non, émanant des établissements d'enseignement et de recherche français ou étrangers, des laboratoires publics ou privés.

# Optical and electrical diagnostics in an iodine plasma

IEPC-2019-A-933

*Presented at the 36th International Electric Propulsion Conference  
University of Vienna, Austria  
September 15-20, 2019*

Florian Marmuse\*, Romain Lucken, Cyril Drag,  
Jean-Paul Booth, Anne Bourdon, and Pascal Chabert  
*Laboratoire de Physique des Plasmas, CNRS, École polytechnique, Sorbonne Université,  
université Paris-sud. Route de Saclay, 91128 Palaiseau CEDEX, France*

Ane Aanesland  
*ThrustMe, Verrières-le-Buisson, France*

Iodine is being studied as the next generation propellant for electric propulsion: dense, stored as a solid, it is also much cheaper than xenon for similar mass and ionization potential. Iodine plasmas are more complex and less studied than noble gases plasmas, leaving electric propulsion engineers with few models and diagnostics in their toolkits. Here we present three experimental diagnostics deployed on a low pressure Radio-Frequency inducted Inductively Coupled iodine plasma discharge. Two optical diagnostics are used to probe the I atom and the I<sub>2</sub> molecule: **classical** absorption at 1.3 μm gives the line-of-sight integrated temperature and density of I; low-resolution broadband absorption spectroscopy between 480 and 500 nm gives the line-of-sight integrated density of I<sub>2</sub>. A Langmuir probe is used to determine the electron temperature and the negative species density at the centre of the plasma, provided that the data are treated by taking in consideration the electronegativity of the plasma. Comparisons with a global model derived from Grondein et al., 2016 ~~tends to suggest~~, that the recombination coefficient at the walls is underestimated for our setup.

## Nomenclature

$I$  = amplitude of the RF current  
 $\tilde{\nu}$  = wavenumber in inverse cm  
 $\lambda$  = wavelength in nm  
 $\sigma$  = cross section in m<sup>2</sup>  
 $d$  = optical depth, dimensionless

---

\*PhD student, florian.marmuse@lpp.polytechnique.fr

## I. Introduction

THE experimental measurements are done in the PEGASES ion source [1], with no acceleration stage. The complete PEGASES thruster features an additional acceleration stage made of two grids, dedicated to the acceleration of positive ions, or both positive and negative ions. The ionization chamber is a 12 x 12 x 8 cm rectangle and is closed by a floating aluminium plate of 2 mm thickness with a 1 cm diameter hole in its center. The plasma is generated via a 4 MHz flat coil separated from the chamber by a 3 mm thick ceramic plate. The PEGASES chamber is equipped with optical access on each side of 8 cm \* 5 mm. The windows installed are mounted at Brewster angle to cancel reflection. This has also the side effect of having the glass farther from the plasma-limiting window deterioration. The vacuum setup is detailed Figure 1.

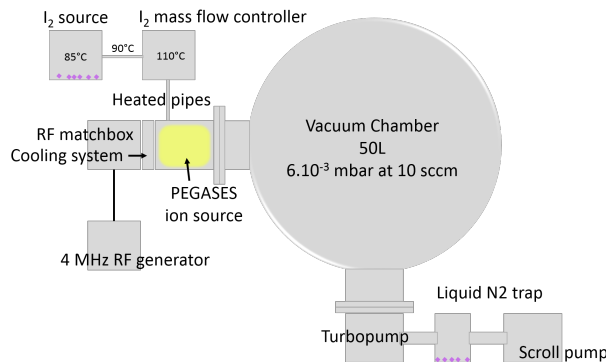


Figure 1: Vacuum setup: PEGASES adapted for iodine plasmas

The power discharge detailed in the entire paper corresponds to the power sent by the RF generator, from which is subtracted the reflected power and the power lost in the coil with the method from Valery Godyak detailed in [2]. The power lost in the antenna is shown to be equal to  $0.24 I^{2.5}$  with  $I$  the current amplitude and the 2.5 factor showing a strong self-inductance effect.

The objective of the measurements presented here are to characterize the iodine plasma created in the chamber and compare to global models derived from [3]. The current work aims at measuring the density of I, I<sub>2</sub> and electrons, as well as the temperature of I and electrons.

## II. I absorption at 1.3 micron

THE transition probed is the fine structure of the fundamental state of the I atom. It's a weak magnetic dipole transition coupled to a electric quadrupole transition, whose cross section and hyperfine line strengths have been calculated by Ha et al., 1995 [4]. The 6 observed hyperfine lines are detailed Figure 2. This laser absorption experiment leads to a line-of-sight integrated value of the density and temperature of the I atoms in the plasma. One characteristic of this experiment is the very low absorption of the transition. Even with nine passes through Brewster-angle windows, the data presented here are close to the limit signal to noise ratio and a cavity-ring down spectroscopy absorption has been tested for lower pressure, without good results yet due to unstable plasmas at very low pressure.

### A. Setup

THE optical setup is shown Figure 3. A tunable diode is used to probe the plasma. The light beam is directed to pass 9 times in the plasma and is collected by a photodiode. The diode is scanned in current, leading to a modulation in wavelength with time. No lambdameter is used to measure the current wavelength, hence the wavelength range of the spectra is recalibrated: it has been shown that the wavelength emitted by the laser is quadratic with time, hence measuring a set of three or more peaks allows to recalibrate the whole spectrum, using peak location from the literature. A Fabry-Perot interferometer is also installed and used to verify the calibration or to recalibrate spectra with less than three peaks.

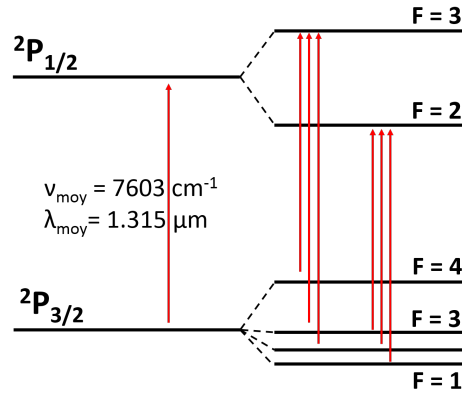


Figure 2: Levels of the hyperfine structure in the fundamental state of the I atom probed in the experiment

## B. Method

ONCE recalibrated, the spectrum is **fitter** with Doppler-broadened Gaussian peaks. The analysis presented here is done on the three smaller peaks between  $7602.6 \text{ cm}^{-1}$  and  $7602.75 \text{ cm}^{-1}$  ( $1.315 \text{ }\mu\text{m}$ ). Each data point comes from the acquisition of two spectra, one with plasma and a reference spectrum without plasma, both of them shown Figure 4a. The laser diode's wavelength is swept in time by changing the diode current. Therefore, an increase in time along the x-axis corresponds to an increase in intensity and an increase in wavelength. The increase in intensity and possible non-linearity are corrected by dividing the data by the reference spectrum, giving transmission, that is plotted against recalibrated wavenumber **on** Figure 4b. The reference spectrum is not taken at the same time as the other spectrum, resulting in a transmission sometimes not being equal to 1. The optical depth is calculated using the classical formula (1), where  $n$  is the density of absorbing species,  $\sigma$  the cross section and  $l$  the path length in the absorbing medium.

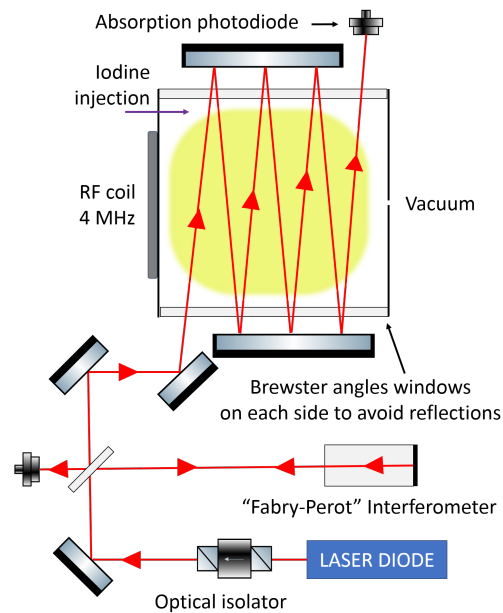


Figure 3: Optical setup with the PEGASES Ion Source. The setup was later modified to make 9 passes through the plasma.

$$d(\nu) := nl\sigma(\nu) = -\ln\left(\frac{I}{I_0}\right) \quad (1)$$

The baseline  $d_\alpha$  is characterized by a unknown third-order polynomial during the fit process. The optical depth  $d_{\text{plasma}}$  is described as the sum of three gaussian peaks. The final fit is

$$d = d_\alpha(\omega) + \sum_1^3 d_i(\omega)$$

Each peak is written

$$d_i(\omega) = B_i \exp\left(-\frac{(\omega - \omega_{0,i})^2}{\alpha T_i}\right)$$

With  $\alpha$  kept constant, and defined as

$$\alpha = \frac{2k\omega_0^2[\text{rad s}^{-1}]}{mc^2} = \frac{8k\pi^2 10^4 \tilde{\nu}^2[\text{cm}^{-1}]}{m}$$

The density for each peak is then derived by dividing the peak area  $B_i\sqrt{\pi\alpha T}$  by the path length  $l$ , the mean angular frequency  $\omega_0$ , the total cross section  $G$  and the line strength within the hyperfine structure  $Q_i$ .

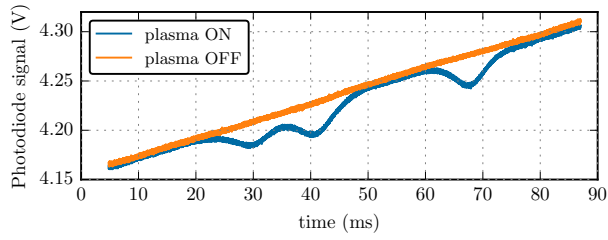
$$n_i = \frac{B\sqrt{\pi\alpha T}}{GQ_i l \omega_0} = \frac{B}{GQ_i l} \sqrt{\frac{2k\pi T}{mc^2}}$$

### C. Results

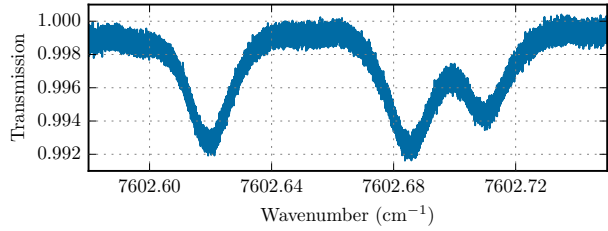
In the next plots, the temperatures and densities plotted are the average between the lines  $3 \leftarrow 3$  and  $3 \leftarrow 4$ . This choice ~~has been~~ made for several reasons: both lines are intense, they give matching results in the preliminary analysis, they can be taken simultaneously in a single measurement. The displayed error bars are the discrepancy between those two lines.

**TEMPERATURE** Figure 5 shows the temperatures for four different values of pressure: it can be seen that temperature increases with pressure, ~~and this increases correspond to an ideal gas behavior.~~ The measured temperature does not depend on discharge power. The error bars are rather small and give confidence in the measurements.

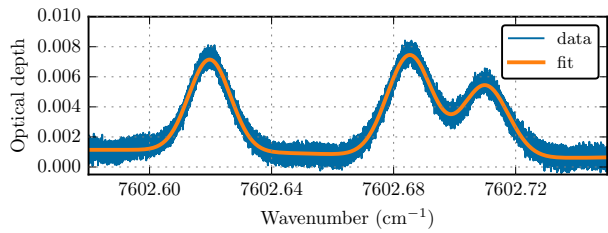
**DENSITY** Figure 6 shows the densities for the same four functioning points and, as expected, the densities increases proportionally with pressure. It also shows that the densities are nearly constant with discharge power, indicating that the plasma has reached a steady state where the dissociation of  $\text{I}_2$  is balanced by other recombination phenomena.



(a) Raw data and reference spectrum



(b) Transmission



(c) Experimental optical depth and fit with a sum of three independent gaussian Doppler broadening curves

Figure 4: Example data analysis for I absorption at  $1.3\ \mu\text{m}$  on three absorption peaks.

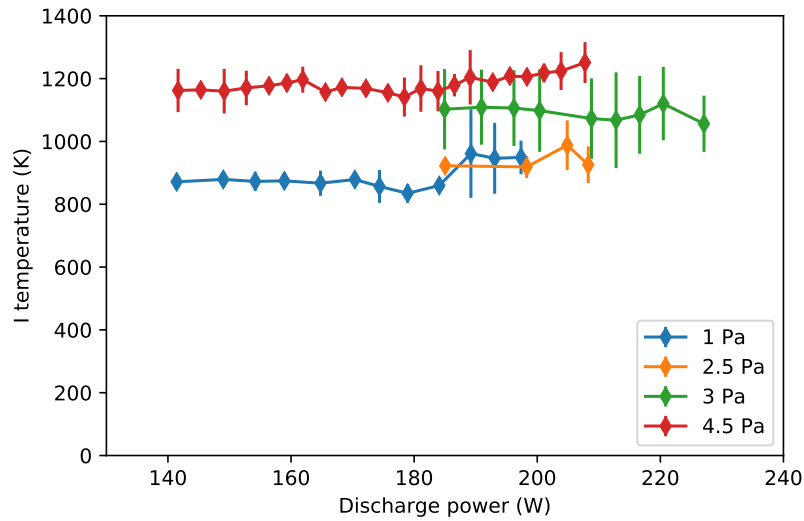


Figure 5: Temperature evolution of the plasma for different discharge power and pressure. The experiments have been performed at constant mass flow rate and the pressure displayed is the average pressure over the data set.

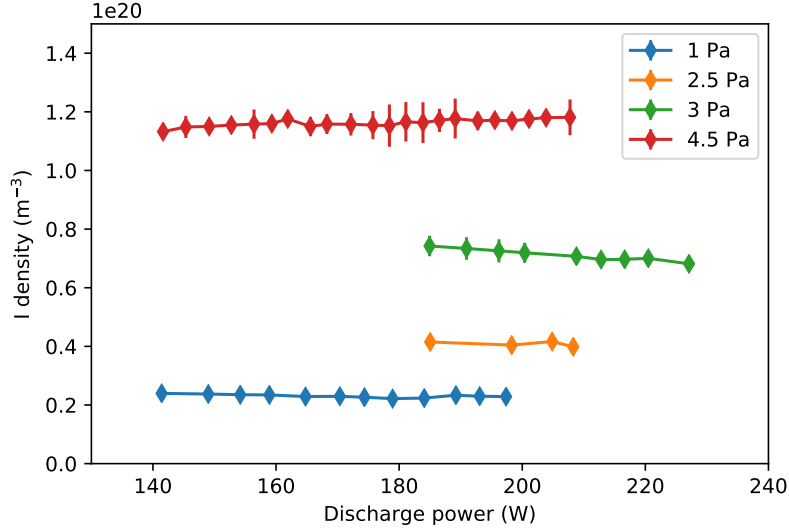
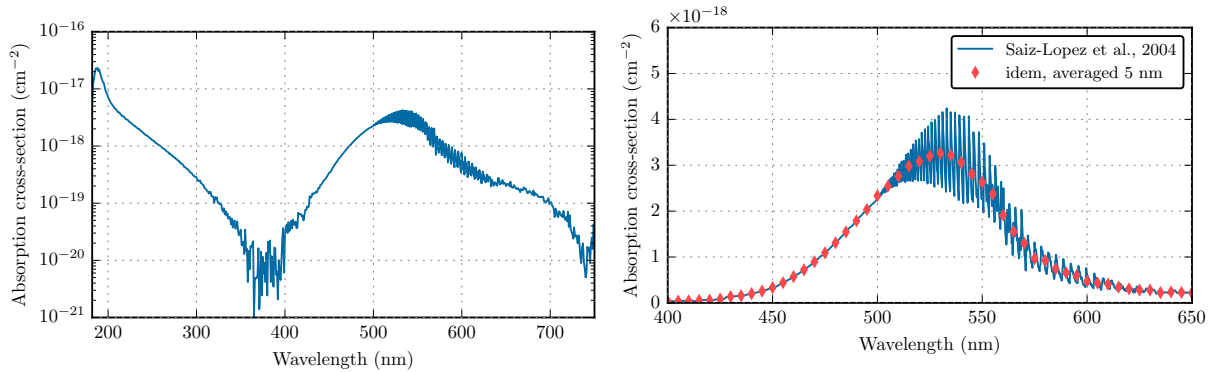


Figure 6: Density evolution of the plasma for different discharge power and pressure. The experiments have been performed at constant mass flow rate and the pressure displayed is the average pressure over the data set.

### III. I<sub>2</sub> broadband absorption between 480 and 500 nm

THIS second experiment aims at measuring the line-of-sight integrated density of the I<sub>2</sub> molecule. The absorption cross sections of I<sub>2</sub> are shown Figure 7. Figure 7a shows two main absorption bands, under 300 nm and from 450 nm to 700 nm. The structure of the second band is detailed Figure 7b: an absorption continuum is present until 500 nm and a second part presents a strong rovibrational structure until 650 nm. The data are from Saiz-Lopez et al., 2004 [5].



(a) Absorption cross sections of the I<sub>2</sub> molecule between 180 and 750 nm. (b) Absorption cross sections of the I<sub>2</sub> molecule between 400 and 650 nm, with a 5nm average to smooth the rovibrational structure.

Figure 7: Cross section data for I<sub>2</sub> from Saiz-Lopez et al., 2004 [2]

#### A. Setup

The optical setup is shown in Figure 8. Light from the tungsten-halogen bulb in the DH-2000 UV-VIS-NIR lamp from Mikropack-OceanOptics is injected in the plasma through an optical fiber. After reflection on a flat mirror on the other side of the PEGASES ion source, the light is collected through a collector and

a optical fiber by a FLAME-S-UV-VIS-ES spectrometer from OceanOptics. The spectrometer has a range from 200 nm to 850 nm and a resolution around 0.5 nm.

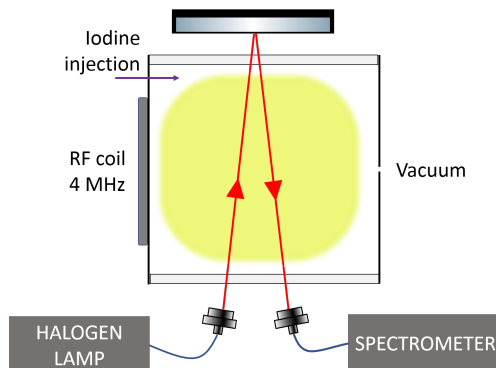


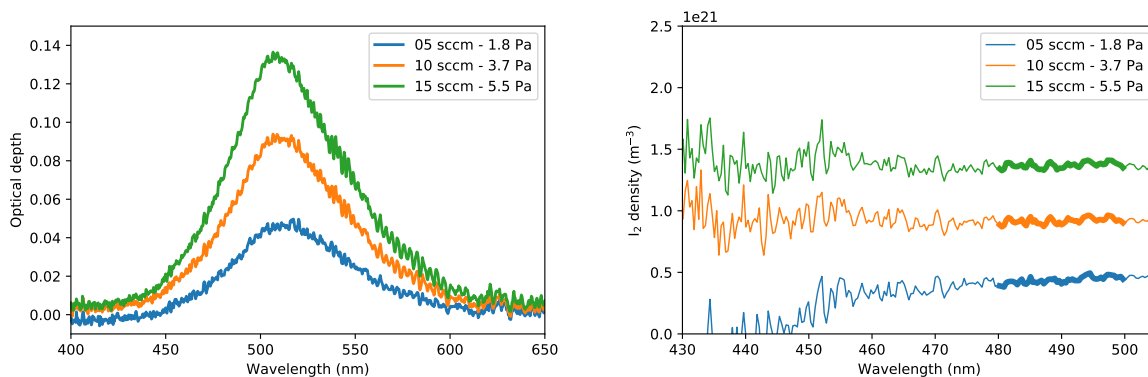
Figure 8: Optical setup for the broadband  $I_2$  absorption experiment. The windows are still Brewster angle windows.

## B. Method

Using the classical absorption formula, the  $I_2$  density can be deduced from the measured optical depth if the cross-section is known:

$$I(\lambda) = I_0(\lambda) \exp(-nL\sigma(\lambda))$$

Theoretically, the entire wavelength range could be used for the measurement. Practically speaking, the measured absorption does not fit the literature data outside the continuum located between 450 and 500 nm, whether or not a plasma is turned on. The method has been experimented in PEGASES filled with pure  $I_2$ , with no plasma, for validation, as shown Figure 10.  $I_2$  absorption is measured for a certain flow of  $I_2$ . The pressure is monitored with a capacitance manometer pressure probe. Figure 9a shows the optical depth in the spectral region of interest for the different pressures. A wide absorption band can be seen, more important as the pressure goes up as expected. Figure 9b shows the densities obtained in the reduced spectral range 430 nm to 505 nm - the continuum - when dividing each data point by the corresponding cross section from [2]. The density is not constant over the entire continuum as it should be, the noise and decrease under 450 nm being most probably related to the strong decrease both in intensity of the lamp and of the cross section. For future plots, the value plotted is the average over the 480 nm to 500 nm range.



(a) Optical thickness of  $I_2$  in the chamber with no power injection.

(b)  $I_2$  density obtained by dividing the optical depth by the cross sections, plasma OFF

Figure 9: Data analysis example for the broadband spectroscopy measurement, plasma OFF.

Figure 10 shows the density of  $I_2$  measured with this method against the pressure measured. It can be seen that the linearity is respected, and the data can be very well fitted with a perfect gas' law ( $P = nkT$ ) with  $T = 311\text{ K}$ , in agreement with the experimental conditions.

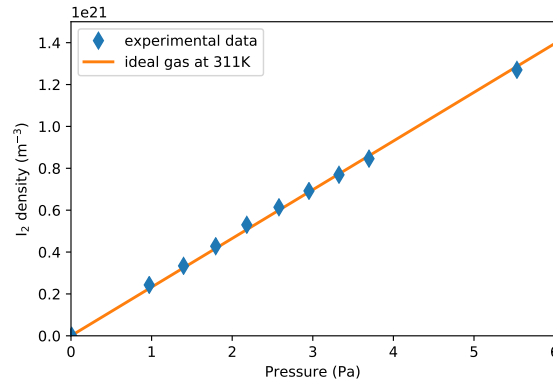


Figure 10: Measured  $I_2$  density and pressure correspond to the behavior of an ideal gas at 311K

### C. Results

With plasma turned on, the shape of the absorption band outside the continuum is modified, mainly because of the population of the vibrationnaly excited levels. The shape of the continuum between 480 and 500 nm is still coherent, providing a constant density over this wavelength range. Figure 11 shows the results of a measurement campaign performed at 5 different mass flow rates in the PEGASES thruster equipped with its Brewster-angle windows. The lamp does two passes in the plasma. One can see that the density of  $I_2$  is rather constant with the discharge power at the power **probed**. The  $I_2$  density is increasing with mass flow rate, as more iodine is brought in the thruster.

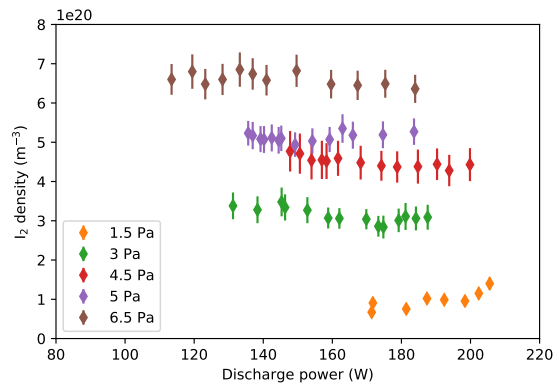


Figure 11: Measured  $I_2$  density for different discharge powers and pressures. The experiment was done at constant mass flow rate and the pressure displayed is an average pressure over the data set.

## IV. Langmuir probe measurements

ELECTRONIC density and temperature are often derived from Langmuir probe measurements in this kind of plasma. A two-pin Langmuir probe has been placed in the plasma. Each pin is made of tungsten, 200 microns in diameter and 3.9 mm in length. Both pins are connected to the outside measurement system VGPS through a two-hole glass capillary. The results shown here are preliminary results computed with the OML method neglecting the electronegativity of the plasma.

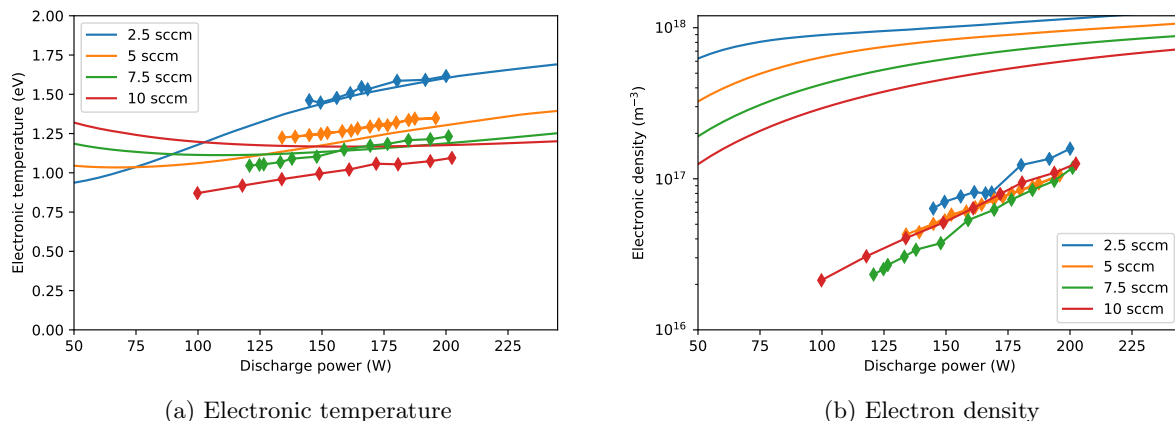


Figure 12: Preliminary data from the Langmuir probe measurements, using the OML method and neglecting the electronegativity of the plasma. The full lines are outputs from the global model.

The global model parametered in mass flow rate gives a pressure slightly different from the experiments. Once the grid transparency adjusted (2% instead of 1%) so that the pressure output roughly matches the measured pressure, a good agreement is found for the electronic temperature, but the measured electronic density is one order of magnitude too low.

## V. Discussion and comparisons with a global model

### A. Estimation of $I_2$ dissociation: experiment

If we consider that the pressure indicated by the capacitance manometer is the neutral partial pressure corresponding to I and  $I_2$ , we have now three information, one of them redundant, to estimate the dissociation of  $I_2$  in I atoms. Figure 13 shows the ratio between the I partial pressure ( $p_I = n_I k T_I$ ) and the total pressure measured in PEGASES. It shows a dissociation of  $I_2$  around 40% and seemingly slightly increasing with pressure.

The independent measurement of  $I_2$  density at the same pressures and powers is meant to validate the pressure measurement. The results are shown Figure 14 where the cumulative densities are plotted: it shows a dissociation of around 20%.

### B. Line of sight integration and radial profile

One expected strong bias of the current setup is the part of the path that happens within the Brewster angle windows. One path in PEGASES is 12cm in the plasma and 8 in the windows(4cm each side) where no plasma can be seen. The current assumptions made for the analysis here are:

- There is no I atom in the windows, which means that the recombination rate is considered high.
- The  $I_2$  density and temperature are homogeneous in the plasma chamber and in the windows. Previous work have shown that in such a plasma the neutral species are depleted in the bulk and accumulate in the edges. An accumulation of  $I_2$  in the windows and a depletion in the bulk would mean the current plots overestimate the  $I_2$  density in the plasma and underestimate the dissociation.

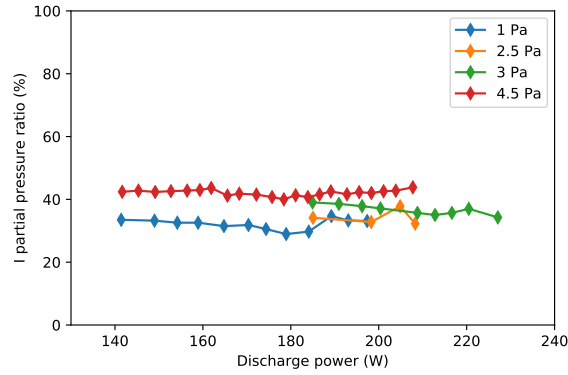


Figure 13: Ratio of I pressure measured with laser absorption over total pressure measured with capacitance manometer

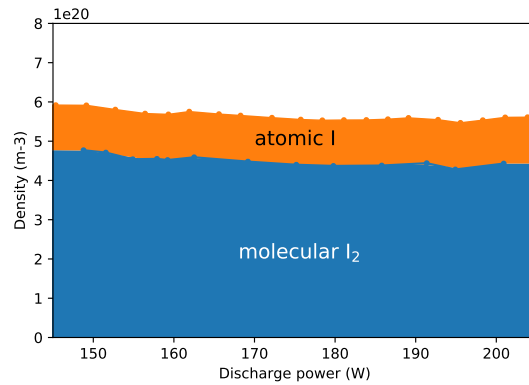
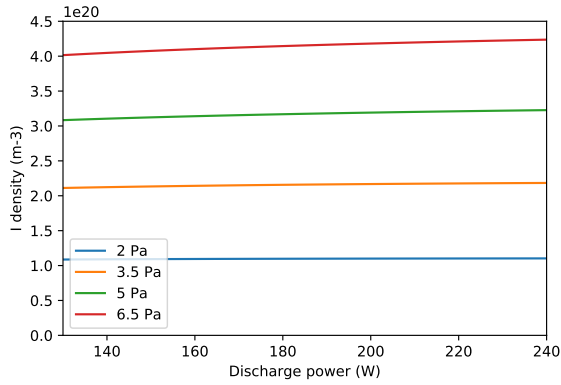


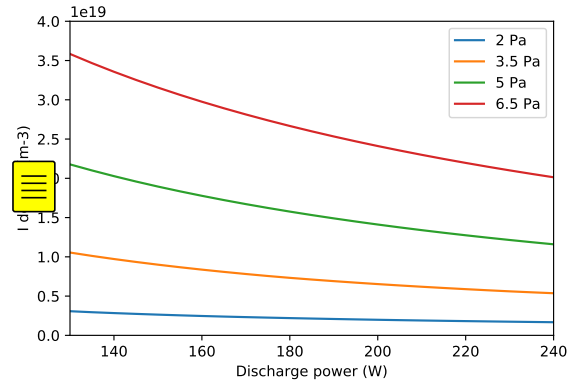
Figure 14: I density measured with laser absorption and I<sub>2</sub> density measured with broadband absorption

### C. Global model

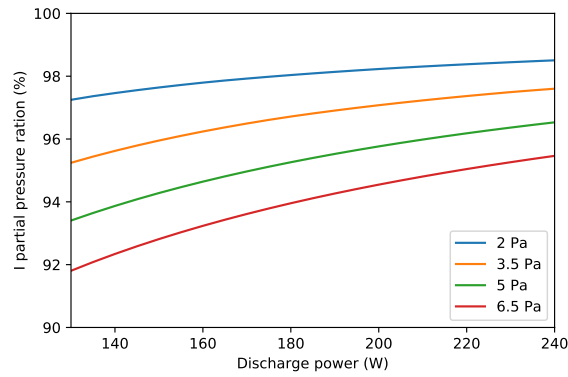
The global model simulation, made with a model derived from [3], shows a dissociation over 90%. In particular, the I density is four times higher in the simulation than what is really measured. The I<sub>2</sub> density is 20 times lower in the experiments than in the models. This suggests that the I to I<sub>2</sub> surface recombination factor is ~~way more important~~ that the factor 0.02 used in [3].



(a) I density expected from the global model



(b) I<sub>2</sub> density expected from the global model



(c) Corresponding dissociated fraction

Figure 15: Outputs of the global model regarding I and I<sub>2</sub> densities

## References

- [1] Leray, Gary. 2009. “PEGASES: Plasma Propulsion with Electronegative Gases.” Ecole Polytechnique X. <https://pastel.archives-ouvertes.fr/pastel-00005935/>.
- [2] Godyak, V. A., R. B. Piejak, and B. M. Alexandrovich. 1999. “Experimental Setup and Electrical Characteristics of an Inductively Coupled Plasma.” *Journal of Applied Physics* 85 (2): 703–12. <https://doi.org/10.1063/1.369150>.
- [3] Grondein, P., T. Laffeur, P. Chabert, and A. Aanesland. 2016. “Global Model of an Iodine Gridded Plasma Thruster.” *Physics of Plasmas* 23 (3): 033514. <https://doi.org/10.1063/1.4944882>.
- [4] Tae-Kyu Ha, Yabai He, Jörg Pochert, Martin Quack, Roland Ranz, Georg Seyfang, and Ioannis Thanopoulos. 1995. “Absolute Integrated Band Strength and Magnetic Dipole Transition Moments in the  $2P_{3/2} - P_{1/2}$  Fine Structure (with Hyperfine Structure) Transition of the Iodine Atom: Experiment and Theory.” *Berichte Der Bunsengesellschaft Für Physikalische Chemie* 99 (3): 384–92.
- [5] Saiz-Lopez, A, R W Saunders, D M Joseph, S H Ashworth, and J M C Plane. 2004. “Absolute Absorption Cross-Section and Photolysis Rate of  $I_2$ .” *Atmos. Chem. Phys.*, 8. <https://doi.org/10.5194/acp-4-1443-2004>.